2012

Nonlinear analysis of biaxially loaded high strength rectangular concrete-filled steel tubular slender beam-columns, part I: theory

Qing Quan Liang
University of Victoria

Vipulkumar Ishvarbhai Patel
University of Victoria

Muhammad N. S Hadi
University of Wollongong, mhadi@uow.edu.au

Publication Details

Liang, Q., Patel, V. Ishvarbhai. & Hadi, M. N. S. (2012). Nonlinear analysis of biaxially loaded high strength rectangular concrete-filled steel tubular slender beam-columns, part I: theory. In J. Liew & S. Lee (Eds.), Proc. of the 10th Intl. Conf. on Advances in Steel Concrete Composite and Hybrid Structures (pp. 403-410). Singapore: Research Publishing.

Nonlinear analysis of biaxially loaded high strength rectangular concrete-filled steel tubular slender beam-columns, part I: theory

Abstract

This paper presents a new numerical model for the nonlinear inelastic analysis of biaxially loaded high strength thin-walled rectangular concrete-filled steel tubular (CFST) slender beam-columns. The numerical model considers the effects of progressive local buckling, initial geometric imperfections, high strength materials and second order. The accurate fiber element method is used to model the inelastic behavior of composite cross-sections. Theoretical models are developed that simulate the load-deflection responses and strength envelopes of thin-walled rectangular CFST slender beamcolumns under biaxial loads. New computational algorithms based on the M?? ller's method are developed to adjust the depth and orientation of the neutral axis and the curvature at the columns ends to obtain nonlinear solutions. The numerical model developed is shown to be an accurate and efficient computer simulation and design tool for biaxially loaded high strength thin-walled rectangular CFST slender beam-columns with large depth-to-thickness ratios. The verification and applications of the numerical model are described in a companion paper.

Keywords

rectangular, strength, high, loaded, biaxially, analysis, nonlinear, part, columns, beam, slender, tubular, theory, steel, i, filled, concrete

Disciplines

Engineering | Science and Technology Studies

Publication Details

Liang, Q., Patel, V. Ishvarbhai. & Hadi, M. N. S. (2012). Nonlinear analysis of biaxially loaded high strength rectangular concrete-filled steel tubular slender beam-columns, part I: theory. In J. Liew & S. Lee (Eds.), Proc. of the 10th Intl. Conf. on Advances in Steel Concrete Composite and Hybrid Structures (pp. 403-410). Singapore: Research Publishing.

Nonlinear Analysis of Biaxially Loaded High Strength Rectangular Concrete-Filled Steel Tubular Slender Beam-Columns, Part I: Theory

Qing Quan Liang; Vipulkumar Ishvarbhai Patel
School of Engineering and Science
Victoria University, PO Box 14428, Melbourne, VIC 8001, Australia
qing.liang@vu.edu.au; vipulkumar.patel@live.vu.edu.au

Muhammad N. S. Hadi
School of Civil, Mining and Environmental Engineering
University of Wollongong, Wollongong, NSW 2522, Australia
mhadi@uow.edu.au

Abstract

This paper presents a new numerical model for the nonlinear inelastic analysis of biaxially loaded high strength thin-walled rectangular concrete-filled steel tubular (CFST) slender beam-columns. The numerical model considers the effects of progressive local buckling, initial geometric imperfections, high strength materials and second order. The accurate fiber element method is used to model the inelastic behavior of composite cross-sections. Theoretical models are developed that simulate the load-deflection responses and strength envelopes of thin-walled rectangular CFST slender beam-columns under biaxial loads. New computational algorithms based on the Müller's method are developed to adjust the depth and orientation of the neutral axis and the curvature at the columns ends to obtain nonlinear solutions. The numerical model developed is shown to be an accurate and efficient computer simulation and design tool for biaxially loaded high strength thin-walled rectangular CFST slender beam-columns with large depth-to-thickness ratios. The verification and applications of the numerical model are described in a companion paper.

1. Introduction

Although high strength thin-walled rectangular concrete-filled steel tubular (CFST) slender beam-columns are frequently used in high-rise composite buildings, efficient analysis and design methods for these columns have not been developed owing to the lack of experimental and numerical research on this type of composite columns. The use of the high strength thin-walled rectangular steel tubes leads to economical designs but may cause local buckling that reduces the ultimate strengths of CFST columns. The effects of local buckling have not been considered in existing methods for the inelastic stability analysis of thin-walled CFST slender beam-columns under biaxial bending. These methods may overestimate the ultimate strengths of thin-walled CFST beam-columns. This paper aims to develop a numerical model for simulating the local and global buckling behavior of high strength thin-walled rectangular CFST slender beam-columns under combined axial load and biaxial bending.

Test results indicated that the confinement effect provided by the rectangular steel tube did not increase the compressive strength of the concrete core in a rectangular CFST column but significantly improved its ductility (Furlong, 1967; Knowles and Park, 1969; Schneider, 1998;

Proc. of the 10th Intl. Conf. on Advances in Steel Concrete Composite and Hybrid Structures
Edited by J Y Richard Liew and Siew Chin Lee

ISBN: 978-981-07-2615-7 :: doi:10.3850/978-981-07-2615-7_116

Han, 2002; Fujimoto *et al.* 2004). Ge and Usami (1992) tested six thin-walled square CFST columns with and without internal stiffeners under cyclic compressive loads. It was observed that thin steel plates buckled locally outward. Bridge and O'Shea (1998) conducted tests to determine the strengths of axially loaded short thin-walled CFST columns with width-to-thickness ratios ranging from 37 to 130. Liang *et al.* (2007) proposed a set of effective strength and width formulas for the design of steel plates in thin-walled CFST beam-columns.

Very few experimental studies on CFST slender beam-columns under biaxial loads have been conducted. Bridge (1976) carried out tests on normal strength square CFST slender beam-columns under axial load and biaxial bending. The experimental behavior of biaxially loaded rectangular CFST slender beam-columns was examined by Shakir-Khalil and Zeghiche (1989) and Shakir-Khalil and Mouli (1990).

Analytical and numerical models have been developed by researchers for determining the behavior of CFST columns. Lakshmi and Shanmugam (2002) presented a semi-analytical method for modeling the behavior of rectangular CFST slender beam-columns under biaxial bending. However, the semi-analytical model does not account for the effects of concrete tensile strength, steel strain hardening and local buckling on the strength and ductility of rectangular CFST beam-columns. Liang (2009) and Patel *et al.* (2012a) developed numerical models for the nonlinear analysis of biaxially loaded thin-walled CFST short columns and uniaxially loaded slender beam-columns with local buckling effects.

In this paper, a new numerical model is presented for simulating the behavior of high strength thin-walled rectangular CFST slender beam-columns under axial load and biaxial bending (Liang *et al.* 2012). The fiber element analysis of cross-sections is described that incorporates the effects of local and post-local buckling of steel tube walls under stress gradients. Computational procedures for modeling the load-deflection responses and strength envelopes of thin-walled CFST slender beam-columns under biaxial loads are given. The verification and applications of the numerical model are provided in a companion paper (Patel *et al.* 2012b).

2. Fiber Element Analysis of Sections

The cross-section of a rectangular CFST beam-column is discretized into fiber elements as depicted in Fig. 1. Each fiber element can be assigned either steel or concrete material properties. The numerical model assumes that plane section remains plane after deformation. This leads to a linear strain distribution through the depth of the section. The fiber strains can be calculated from the curvature (ϕ), the depth (d_n) and orientation (θ) of the neutral axis. For $0^\circ \le \theta < 90^\circ$, the concrete and steel fiber strains can be calculated by the following equations proposed by Liang (2009):

$$y_{n,i} = \left| x_i - \frac{B}{2} \right| \tan\theta + \left(\frac{D}{2} - \frac{d_n}{\cos\theta} \right) \tag{1}$$

$$\varepsilon_i = \begin{cases} \phi \left| y_i - y_{n,i} \right| \cos\theta & \text{for } y_i \ge y_{n,i} \\ -\phi \left| y_i - y_{n,i} \right| \cos\theta & \text{for } y_i < y_{n,i} \end{cases} \tag{2}$$

where B and D are the width and depth of the rectangular column section respectively, x_i and y_i are the coordinates of fiber i and ε_i is the strain at the ith fiber element and $y_{n,i}$ is the distance from the centroid of each fiber to the neutral axis. For $\theta = 90^\circ$, the beam-column is subjected to uniaxial bending and fiber strain calculation is given by Liang (2009). Fiber stresses are calculated from fiber strains using the material uniaxial stress-strain relationships.

Internal axial force and moments acting on a cross-section are determined as stress resultants in the cross-section (Liang 2009).

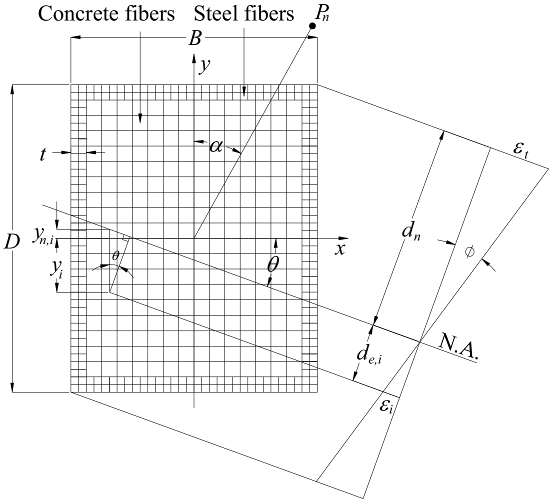

Figure 1: Fiber element discretization of CFST column section

3. Material Constitutive Models for Concrete and Structural Steels

As noted that the confinement effect increases the ductility of the concrete core in a rectangular CFST column. This effect is considered in the stress-strain curve for concrete in rectangular CFST columns suggested by Liang (2009) as shown in Fig. 2(a). This constitutive law for concrete is adopted in the present numerical model.

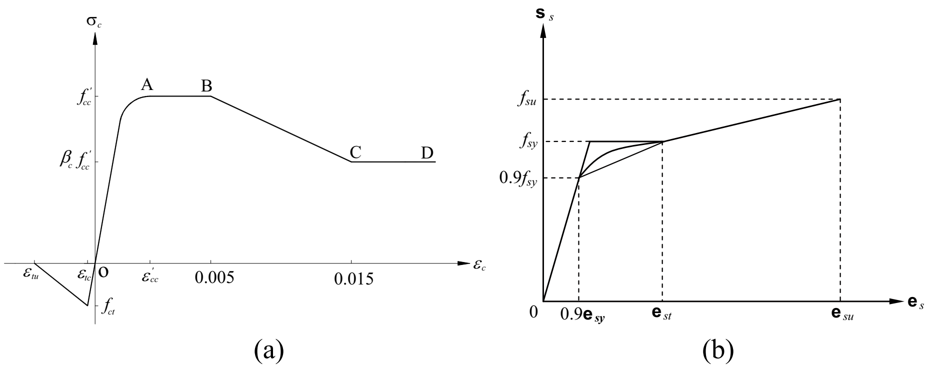

Figure 2: Material models: (a) Concrete (b) Structural steels

The part OA of the stress-strain curve is modeled using the equations suggested by Mander *et al*. (1988) as

$$\sigma_c = \frac{f'_{cc}\lambda\left(\varepsilon_c/\varepsilon'_{cc}\right)}{\lambda - 1 + \left(\varepsilon_c/\varepsilon'_{cc}\right)^{\lambda}} \tag{3}$$

$$\lambda = \frac{E_c}{E_c - \left(f'_{cc}/\varepsilon'_{cc}\right)} \tag{4}$$

$$E_c = 3320\sqrt{f'_{cc}} + 6900 \quad \text{(MPa)} \tag{5}$$

where σ_c is the compressive concrete stress, f'_{cc} is the effective compressive strength of concrete, ε_c is the concrete compressive strain and ε'_{cc} is the strain at f'_{cc} and E_c is the Young's modulus of concrete. The strain ε'_{cc} is between 0.002 and 0.003 depending on the effective compressive strength of concrete (Liang, 2009).

The parts A to D of the stress-strain curve for concrete as shown in Fig. 2(a) is modeled by equations given by Liang (2009) as

$$\sigma_c = \begin{cases} f'_{cc} & \text{for } \varepsilon'_{cc} < \varepsilon_c \le 0.005 \\ \beta_c f'_{cc} + 100(0.015 - \varepsilon_c)(f'_{cc} - \beta_c f'_{cc}) & \text{for } 0.005 < \varepsilon_c \le 0.015 \\ \beta_c f'_{cc} & \text{for } \varepsilon_c > 0.015 \end{cases} \tag{6}$$

where β_c reflects the confinement effect on the concrete ductility and it is equal to 1.0 when the D/t ratio is less than 24 and is taken as 0.5 when the D/t ratio is greater than 48. For D/t ratio between 24 and 48, β_c is determined as $(1.5 - D/48t)$ as suggested by Liang (2009). The effective compressive strength of concrete (f'_{cc}) is influenced by the column size, the quality of the concrete and the loading rates. In this study, f'_{cc} is calculated as $\gamma_c f'_c$. The reduction factor γ_c was proposed by Liang (2009) to account for the column size effect on the compressive strength of concrete and is taken as $\gamma_c = 1.85\, D_c^{-0.135}$, where D_c is the diameter of the concrete core and taken as the larger of $(B - 2t)$ and $(D - 2t)$ for a rectangular cross-section.

The stress-strain relationship for concrete in tension as depicted in Fig. 2(a) assumes that the tension stress increases linearly with an increase in tensile strain up to concrete cracking. After concrete cracking, the tensile stress decreases linearly to zero as the concrete softens. The ultimate tensile strain is taken as 10 times of the strain at cracking.

Steel tubes are usually made of high strength structural steel, cold-formed steel or mild structural steel. For mild structural steels, an idealized tri-linear stress-strain curve is assumed as shown in Fig. 2(b). An idealized linear-rounded-linear stress-strain curve is used for cold-formed steels. The rounded part in the curve can be modeled by a formula proposed by Liang (2009). For high strength steels, the rounded part is replaced by a straight line.

4. Local and Post-local Buckling

The effects of local and post-local buckling are taken into account in the numerical model. For a CFST column under axial load and biaxial bending, the steel tube walls may be subjected to compressive stress gradients as depicted in Fig. 3. The formulas proposed by Liang *et al*. (2007) are incorporated in the numerical model to determine the initial local buckling stresses of the steel tube walls under stress gradients. The post-local buckling strength of thin steel plates under uniform or stress gradients as shown in Fig. 3 can be described by the effective width concept. The effective widths b_{e1} and b_{e2} shown in Fig. 3 are given by Liang *et al*. (2007) as

$$\frac{b_{e1}}{b} = \begin{cases} 0.2777 + 0.01019\left(\frac{b}{t}\right) - 1.972\times10^{-4}\left(\frac{b}{t}\right)^2 + 9.605\times10^{-7}\left(\frac{b}{t}\right)^3 & \text{for } \alpha_s > 0.0 \\ 0.4186 - 0.002047\left(\frac{b}{t}\right) + 5.355\times10^{-5}\left(\frac{b}{t}\right)^2 - 4.685\times10^{-7}\left(\frac{b}{t}\right)^3 & \text{for } \alpha_s = 0.0 \end{cases} \tag{7}$$

$$\frac{b_{e2}}{b} = (1+\phi)\frac{b_{e1}}{b} \tag{8}$$

where $\phi = 1 - \alpha_s$ and α_s is the stress gradient coefficient which is the ratio of the minimum edge stress σ_2 to the maximum edge stress σ_1 applied to the plate.

The effective strength concept can also be used to describe the post-local buckling behavior of thin steel plates. The ultimate strengths of steel plates under a stress gradient greater than zero are given by Liang *et al*. (2007) as

$$\frac{\sigma_{1u}}{f_{sy}} = (1 + 0.5\phi)\frac{\sigma_u}{f_{sy}} \qquad (0 \le \phi < 1.0) \tag{9}$$

in which σ_{1u} is the ultimate stress corresponding to the maximum edge stress σ_1 at the ultimate state and σ_u is the ultimate strength of the steel plate under uniform compression (Liang *et al*. 2007).

The progressive post-local buckling is modeled by gradually redistributing the normal stresses within the rectangular steel tube walls based on the stress levels as suggested by Liang (2009). The stresses of steel fibers located within ineffective areas are assigned to a zero value as shown in Fig. 3. After initial local buckling, steel fiber stresses are updated to account for post-local buckling effects.

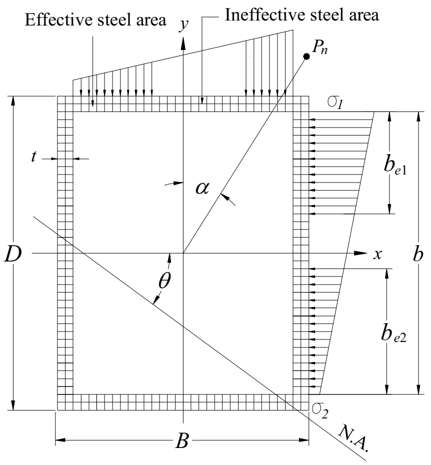

Figure 3: Steel walls under stress gradients

5. Load-deflection Responses

The part-sine displacement function is used to describe the deflected shape of a pin-ended rectangular CFST beam-column. The load-deflection curve is generated by using the deflection control method, in which the deflection at the mid-height of the beam-column is incrementally increased until the deflection limit is reached or the ultimate axial load is obtained. The curvature at the mid-height of the beam-column can be obtained from the displacement function as

$$\phi_m = (\pi/L)^2 u_m \tag{10}$$

where L is the effective length of the beam-column and u_m is the mid-height deflection of the CFST beam-column. The external moment at the mid-height of the beam-column with initial geometric imperfection u_o and under eccentric loading can be calculated by

$$M_{me} = P(e + u_o + u_m) \tag{11}$$

where P is the applied axial load and e the eccentricity of the applied load.

The analysis procedure is given as follows:

(1) Initialize the mid-height deflection of the beam-column: $u_m = \Delta u_m$;
(2) Calculate the curvature ϕ_m at the mid-height of the beam-column;
(3) Adjust the neutral axis depth d_n using the Müller's method;
(4) Calculate the P and M from the moment-curvature relationship;
(5) Repeat Steps (3) to (4) until $|r^a{}_m| = |M_{me} - M_{mi}| < \varepsilon_k$ ($\varepsilon_k = 10^{-4}$);
(6) Adjust the orientation of the neural axis ϕ using the Müller's method;
(7) Calculate $r^b{}_m = \tan\alpha - (M_v - M_x)$;
(8) Repeat Steps (3) to (7) until $|r^b{}_m| < \varepsilon_k$;
(9) Increase the deflection at mid-height of the column by $u_m = u_m + \Delta u_m$;
(10) Repeat Steps (2) to (9) until the ultimate load P_u is obtained or deflection limit is reached.

6. Strength Envelopes

For a given load increment (P_n) applied at a fixed load angle (α), the ultimate bending strength of a slender beam-column is determined as the maximum moment that can be applied to the columns ends. The moment equilibrium is maintained at the mid-height of the beam-column. The external moment at the mid-height of the beam-column is given by

$$M_{me} = M_e + P_n(u_m + u_o) \tag{12}$$

where M_e is the moment at the column ends. The deflection at the mid-height of the slender beam-column can be calculated from the curvature as

$$u_m = (L/\pi)^2 \phi_m \tag{13}$$

To develop the strength envelope, the curvature at the mid-height of the beam-column is gradually increased and the corresponding internal moment is computed by the moment-curvature responses. The curvature at the column ends is adjusted and the corresponding moment at the column ends is calculated until the maximum moment at the column ends is obtained. The axial load is increased and the strength envelope of the slender beam-column can be generated by repeating the above process.

The main steps of the computational procedure are described as follows:

(1) Calculate the ultimate axial load P_{oa} of axially loaded slender beam-column;
(2) Initialize the applied axial load P_n;
(3) Initialize the curvature at the mid-height of the beam-column $\phi_m = \Delta\phi_m$;
(4) Compute the mid-height deflection u_m from the curvature ϕ_m;
(5) Adjust the depth of the neutral axis a_n using the Müller's method;
(6) Calculate resultant force P considering local buckling;
(7) Repeat Steps (5)-(6) until $|r^c{}_m| = |P_n - P| < \varepsilon_k$;
(8) Adjust the orientation of the neutral axis (θ) using the Müller's method;
(9) Repeat Steps (5)-(8) until $|r^b{}_m| = |\tan\alpha - M_y/M_x| < \varepsilon_k$;
(10) Compute the internal resultant moment M_{mi};
(11) Adjust the curvature at the column end ϕ_e using the Müller's method;
(12) Compute the moment M_e at the column ends with local buckling effects;
(13) Repeat Steps (11)-(12) until $r^a{}_m| = |M_{me} - M_{mi}| < \varepsilon_k$;
(14) Increase the curvature at the mid-height by $\phi_m = \phi_m + \Delta\phi_m$;
(15) Repeat Steps (4)-(14) until the ultimate bending strength M_n is obtained;

(16) Increase the axial load by $P_n = P_n + \Delta P_n$, where $\Delta P_n = P_{oa}/10$;
(17) Repeat Steps (4)-(16) until the maximum increment load is reached.

7. Müller's Method Algorithms

The Müller's method algorithms are developed for rectangular CFST slender beam-columns under biaxial bending to obtain nonlinear solutions. The depth (d_n) and orientation (θ) of the neutral axis and the curvature (ϕ_e) at the column ends of a slender beam-column are design variables which are denoted herein by ω. The Müller's method requires three starting values of the design variables ω_1, ω_2 and ω_3. The corresponding force or moment residuals $r_{m,1}$, $r_{m,2}$ and $r_{m,3}$ are calculated based on three initial design variables. The depth and orientation of the neutral axis and the curvature at the column ends are adjusted by using the following equations:

$$\omega_4 = \omega_3 - \frac{2c_m}{b_m \pm \sqrt{b_m^2 - 4a_m c_m}} \tag{14}$$

$$a_m = \frac{(\omega_2 - \omega_3)(r_{m,1} - r_{m,3}) - (\omega_1 - \omega_3)(r_{m,2} - r_{m,3})}{(\omega_1 - \omega_2)(\omega_2 - \omega_3)(\omega_1 - \omega_3)} \tag{15}$$

$$b_m = \frac{(\omega_1 - \omega_3)^2 (r_{m,2} - r_{m,3}) - (\omega_2 - \omega_3)^2 (r_{m,1} - r_{m,3})}{(\omega_1 - \omega_2)(\omega_2 - \omega_3)(\omega_1 - \omega_3)} \tag{16}$$

$$c_m = r_{m,3} \tag{17}$$

The sign of the square room term in the denominator of Eq. (14) is taken as the same as b_m. The values of ω_1, ω_2 and ω_3 and corresponding residual moments $r_{m,1}$, $r_{m,2}$ and $r_{m,3}$ need to switch (Patel *et al*. 2012a).

8. Conclusions

An effective numerical model for simulating the behavior of biaxially loaded high strength thin-walled rectangular CFST slender beam-columns has been presented in this paper. Computational procedures with efficient solution strategies have been proposed that determine the load-deflection responses and strength envelopes of high strength thin-walled rectangular CFST slender beam-columns with local buckling effects. The innovative aspect of the proposed model is the incorporation of the progressive local buckling into the global inelastic stability analysis of thin-walled rectangular CFST slender beam-columns under combined axial load and biaxial bending. This allows for high strength thin-walled rectangular CFST slender beam-columns made of compact, non-compact or slender steel tube sections under biaxial loads to be analyzed and designed. It overcomes the limitations of the existing plastic analysis and design methods that do not permit non-compact or slender steel sections to be used. The verification and applications of the numerical model are given in a companion paper presented by Patel *et al*. (2012b).

9. References

[1] Bridge RQ (1976), *Concrete filled steel tubular columns, School of Civil Engineering, The University of Sydney, Sydney, Australia,* Research Report No. R 283.

[2] Bridge RQ and O'Shea MD (1998), *Behaviour of thin-walled steel box sections with or without internal restraint*, *Journal of Constructional Steel Research,* Vol. 47 No. 1-2, pp. 73-91.

[3] Furlong RW (1967), *Strength of steel-encased concrete beam-columns*, *Journal of the Structural Division*, *ASCE*, Vol. 93 No. 5, pp. 113-124.

[4] Fujimoto T, Mukai A, Nishiyama I and Sakino K (2004), *Behavior of eccentrically loaded concrete-filled steel tubular columns, Journal of Structural Engineering*, *ASCE*, Vol. 130 No. 2, pp. 203-212.

[5] Ge HB and Usami T (1992), *Strength of concrete-filled thin-walled steel box columns: Experiment, Journal of Structural Engineering*, *ASCE*, Vol. 118 No. 11, pp. 3036-3054.

[6] Han LH (2002), *Tests on stub columns of concrete-filled RHS sections*, *Journal of Constructional Steel Research*, Vol. 58 No. 3, pp. 353-372.

[7] Knowles RB and Park R (1969), *Strength of concrete-filled steel tubular columns*, *Journal of Structural Division, ASCE*, Vol. 95 No. 12, pp. 2565-2587.

[8] Lakshmi B and Shanmugam NE (2002), *Nonlinear analysis of in-filled steel-concrete composite columns, Journal of Structural Engineering*, Vol. 128 No. 7, pp. 922-933.

[9] Liang QQ (2009), *Performance-based analysis of concrete-filled steel tubular beam-columns, Part I: Theory and algorithms*, *Journal of Constructional Steel Research*, Vol. 65 No. 2, pp. 363-372.

[10] Liang QQ, Patel VI and Hadi MNS (2012), *Biaxially loaded high-strength concrete-filled steel tubular slender beam-columns, Part I: Multiscale simulation*, *Journal of Constructional Steel Research* (in press).

[11] Liang QQ, Uy B and Liew JYR (2007), *Local buckling of steel plates in concrete-filled thin-walled steel tubular beam-columns*, *Journal of Constructional Steel Research*, Vol. 63 No. 3, pp. 396-405.

[12] Mander JB, Priestley MJN and Park R (1988), *Theoretical stress-strain model for confined concrete*, *Journal of Structural Engineering*, *ASCE*, Vol. 114 No. 8, pp. 1804-1826.

[13] Patel VI, Liang QQ and Hadi MNS (2012a), *High strength thin-walled rectangular concrete-filled steel tubular slender beam-columns*, *Part I: Modeling*, *Journal of Constructional Steel Research*, Vol 70, pp. 377-384.

[14] Patel VI, Liang QQ and Hadi MNS (2012b), *Nonlinear analysis of biaxially loaded high strength rectangular concrete-filled steel tubular slender beam-columns, Part II: Applications*, *the 10th International Conference on Advances in Steel Concrete Composite and Hybrid Structures,* Singapore (accepted).

[15] Schneider SP (1998), *Axially loaded concrete-filled steel tubes*, *Journal of Structural Engineering, ASCE*, Vol. 124 No. 10, pp. 1125-1138.

[16] Shakir-Khalil H and Mouli M (1990), *Further tests on concrete-filled rectangular hollow-section columns*, *The Structural Engineer*, Vol. 68 No. 20, pp. 405-413.

[17] Shakir-Khalil H and Zeghiche J (1989), *Experimental behaviour of concrete-filled rolled rectangular hollow-section columns*, *The Structural Engineer*, Vol. 67 No. 19, pp. 346-353.